

**DETECTION OF ANOMALOUS ELEMENTS, X-RAY AND EXCESS HEAT INDUCED BY CONTINUOUS DIFFUSION OF DEUTERIUM THROUGH MULTI-LAYER CATHODE (Pd/CaO/Pd)**

Yasuhiro IWAMURA, Takehiko ITOH, Nobuaki GOTOH, Mitsuru SAKANO, Ichiro TOYODA and Hiroshi SAKATA

Advanced Technology Research Center, Mitsubishi Heavy Industries, Ltd.  
1-8-1, Sachiura, Kanazawa-ku, Yokohama, 236-8515, Japan,

**Abstract**

A new type of experimental apparatus is developed to induce nuclear reactions by continuous diffusion of deuterium. Ti atoms, which cannot be explained by contamination, were detected on the surface where deuterium atoms passed through on Pd cathodes after electrolysis. A multi-layer cathode (Pd/CaO/Pd) is introduced based on an EINR (Electron Induced Nuclear Reaction) model. Excess heat generations and x-ray emissions were observed for all the cases we tried by the multi-layer cathodes.  $^{57}\text{Fe}/^{56}\text{Fe}$  ratio of Fe atoms detected on the multi-layer cathodes is anomalously larger than natural  $^{57}\text{Fe}/^{56}\text{Fe}$ .

**1. Introduction**

Beginning in 1993, we have researched "cold fusion" phenomena to investigate it as a potential new energy source. At first, we performed gas-loading experiments and suggested that the high diffusion velocity of deuterium, in addition to a high D/Pd ratio, is an important factor for causing nuclear reactions in solids <sup>(1)-(3)</sup>. The authors analyzed electrolyzed Pd samples by a variety of methods <sup>(4)</sup>, and we conjectured that impurities in Pd play essential roles to induce nuclear reactions. The foregoing ideas result in the assumption that necessary conditions to induce nuclear reactions in solids are as follows:

- (i) high D/Pd
- (ii) enough diffusion flux of deuterium
- (iii) the existence of a third element except Pd and deuterium.

A new type of experimental apparatus was developed to induce continuous diffusion under high D/Pd conditions, in which the conditions (i) and (ii) were satisfied. <sup>(5)</sup> A multi-layer cathode composed of a Pd sheet, Pd and CaO complex layer, and Pd thin layer is developed to meet the condition (iii). Ca is introduced into Pd cathode based on an Electron-Induced Nuclear Reaction (EINR) mode <sup>(6)</sup>.

In this paper, experimental results using the continuous diffusion apparatus with both a normal Pd sample and the multi-layer cathodes is described.

## 2. Experimental

Figure 1 shows a cross sectional view of the continuous diffusion experimental apparatus<sup>(3),(6)</sup> An electrolyte of 1M LJOD/D<sub>2</sub>O and a vacuum chamber are separated by a Pd plate with an O-ring gasket (KARLEZ). Deuterium atoms are loaded by electrochemical potential into one side of the Pd sample and released from the other side. With this composition, it is possible to control the state of diffusion of deuterium by applied current or pressure of the vacuum side.

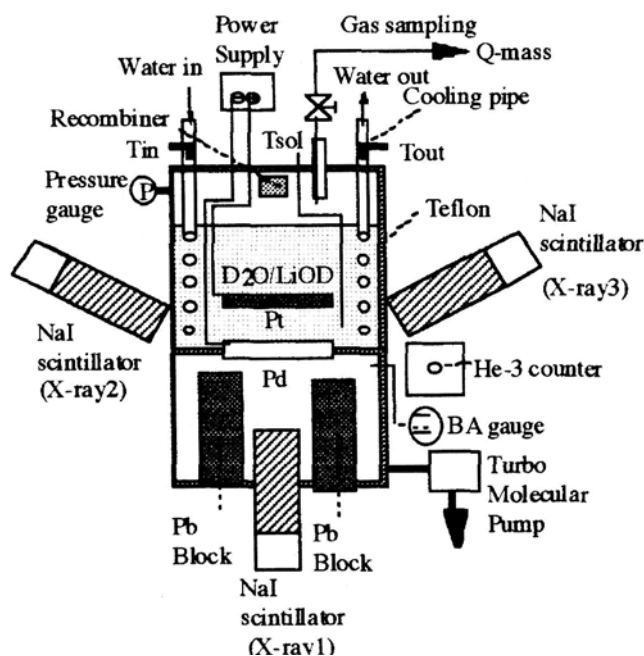


Fig. 1 Continuous Diffusion Experimental Apparatus

Excess heat is estimated by the flow calorimetry method. Heavy water (up to 99.9%) and LiOD (up to 99%) are provided by ISOTEC Inc. The electrolyte side of the apparatus consists of a cathode of Pd plate (25x25x1 mm; 99.9% Tanaka Kikinzoku Kogyo K.K.), a circular shape of anode of platinum mesh ( $\Phi$ 0.5mm; 99.98% Nilaco Co.), a recombiner and a cooling pipe for measurement of excess heat generation.

Pressures of the upper part of electrolyte and vacuum chamber are monitored by a pressure gauge and a BA gauge, respectively. At the beginning of electrolysis, argon gas is filled up at 1 atm in the upper space of the electrolyte.

The recombiner is prepared by electroplating Pt mesh in H<sub>2</sub>PtCl<sub>6</sub> solution. In this apparatus, increase of pressure of the upper part of electrolyte corresponds to absorbed deuterium. Recombiner efficiency is calculated by the analysis of D<sub>2</sub> and O<sub>2</sub> gases in the upper part of the electrolyte using a quadrupole mass spectrometer (AQA-360, ANELVA). Furthermore, temperature of the recombiner is always monitored to make sure that the recombiner works. We confirm that the recombiner works by the temperature and gas analysis. The

usual recombiner efficiency that we measured was  $> 99\%$ .

The cooling pipe is electroplated with gold ( $10\mu\text{m}$  thickness) because Au is resistant to alkaline solution and it has good thermal conductivity. Flow rate of coolant (pure water) is always measured at 2 points: inlet and outlet sides. Two thermocouples each are provided to measure the inlet and outlet temperatures of the water. The Solution, gas, recombiner and environmental temperatures are measured and consistency among these temperatures is always checked. The cell of the electrolyte side of the apparatus is made of Teflon. All experimental parts such as electric wires in the electrolyte side are coated with Teflon. The apparatus and measuring systems are located in a clean room where temperature and humidity are always controlled at constant levels ( $23\pm 1^\circ\text{C}$ ,  $40\pm 5\%$ ). Description on our nuclear measurement is provided in Ref. 5 and 6. The procedure for sample preparation is as follows. Pd plates were washed with acetone and annealed under vacuum condition ( $< 10^{-7}$  torr) at  $900^\circ\text{C}$  for 10 hours. The samples were cooled down to room temperature in furnace and washed with aqua regia (D) for 100 sec to remove impurity on the surface of the Pd samples. In the case of preparing a multi-layer cathode shown in Figure 2, the sample was covered with a complex layer which consisted of CaO and Pd. It was formed by simultaneously sputtering of CaO and Pd with Ar ion beam. Thickness of the layer was set from  $1000\text{\AA}$  to  $3000\text{\AA}$ . A thin Pd layer ( $400\text{\AA}$ ) was formed on it by ion beam sputtering to avoid dissolving CaO into  $\text{D}_2\text{O}/\text{LiOD}$  solution. The complex layer is put at near surface of the electrolyte side because we assume that nuclear reactions occur at the near surface.

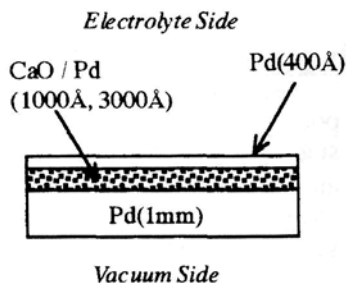


Fig. 2 Structure of a Multi-Layer Cathode

### 3.Results and Discussion

Figure 3 shows the appearance of a normal Pd sample after experiments. Excess heat of about 1W lasted for 1 day in the case of the sample, although x-rays and neutrons were not detected. The black circle of the electrolyte side (surface A) corresponds to the place where deuterium atoms passed through; it is the shape of the Ft anode. Surface B is the place where no deuterium atoms pass through. Similar black circles corresponding to the shape of the anode are observed on multi-layer cathodes. Contrarily, the appearance of the vacuum side of the Pd is the same as before experiments, independent of the deuterium passage.

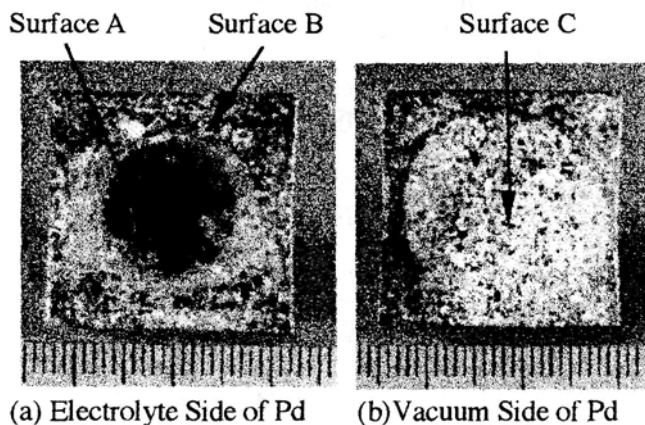


Fig. 3 The Electrolyte and Vacuum Sides of Pd

Figure.4 show the results of EDX (Energy Dispersive X-ray Spectrometry) for the surface A. Ti is clearly seen in the EDX spectrum. The Ti element was confirmed by WDX (wavelength dispersive X-ray spectroscopy), AES (Auger Electron Spectrometry), XPS (X-ray Photoelectron Spectrometry) and ICP-MS (Inductively Coupled Plasma Mass Spectrometry). Those results are consistent with each other. On the other hand, no element except Pd is detected on the surface B and C.

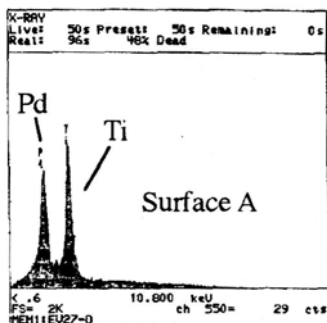


Fig. 4 EDX Spectrum for Surface A

Ti element on the black circle (surface A) was estimated  $21\mu\text{g}$  by the ICP-MS. Maximum quantity of Ti contained in LiOD/D<sub>2</sub>O solution and a Pt anode can be estimated  $3.3\mu\text{g}$ . The LiOD/D<sub>2</sub>O solution was kept for 3 days in the cell before analysis. Mass of Ti in a whole Pd cathode before electrolysis is about  $19\mu\text{g}$ . Therefore, the maximum total mass of Ti is  $22.3\mu\text{g}$  which is the same order of the increased mass of Ti on the surface A.

ICP-MS analysis shows that total mass of Pt or Cu in the electrolyte, Pt and Pd is much larger than Ti. However, Pt and Cu were not detected on the surface A. It is very difficult to consider that only Ti elements were concentrated on the electrolyte surface where deuterium atoms passed through by an ordinary physicochemical process. After experiments, we keep the Pd samples in a

desiccator in the clean room. The possibility of Ti being deposited on the Pd after the experiments is extremely low. Therefore the authors consider that Ti is formed by certain nuclear process in solids.

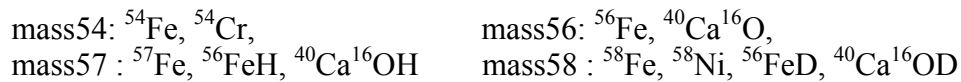
The experimental results using the multi-layer cathodes are summarized in Table 1. All the samples except EV54 belonged to the multi-layer cathodes, although thicknesses of CaO/Pd layers were different. In the table,  $\sigma_x$  denotes standard deviation of the background for each detector. We judge that excess heat is generated only if it exceeds  $3\sigma_H$  of background (Pd-H<sub>2</sub>O system). The excess heat is evaluated by the increase of coolant temperature. Details of excess heat and x-ray analyses are described in Ref. 5 and 6.

Both excess heat generation and x-ray emission were observed for all the multi-layer cathodes as shown in Table 1. Input power ranges from 20W to 40W. X-ray emissions were simultaneously detected by X2 and X3 counters located at the upper side of the Pd. Maximum deviations from mean values of X2 and X3 were shown in the table. Neutron emission of  $22\sigma_n$  was observed only in the case of EV50.

Elements on the surface A of multi-layer cathode after experiments detected by EPMA (Electron Probe Micro Analysis) are shown in the table. The electrolyte, Pt anode, and Pd contain much more Fe, Cu, Si than Ti. The maximum quantities of them in the apparatus easily exceed the quantities of detected elements on the cathode. Several papers<sup>(7)-(9)</sup> report isotope shifts. We apply SIMS (Secondary Ion Mass Spectroscopy) to the detected Fe and show that Fe, at least, can not be explained by contamination.

Mass number ratios (mass57/mass56) are also shown in the table. For some samples, SIMS analyses were performed at several points. The values of the table were obtained by integrating depth profiles. It is noticeable that all the values of mass57/mass56 on multi-layer cathodes are distributed from 0.036 to 0.66; they are larger than 0.023 which is obtained by Fe standard material.

We should consider the following species as the candidates of mass 54, 56, 57 and 58, because a variety of elements on the cathodes are detected by SIMS.



Examples of Depth profile of those mass numbers are shown in Figures 5 and 6. SIMS measurements were performed by MST (Foundation for Promotion of Material Science and Technology of Japan) with Physical Electronics 6600. We see that secondary ion intensity and mass number ratio of EV53 behave anomalously. Especially, mass57/mass 57 reaches 0.8, although natural  $^{57}\text{Fe}/^{56}\text{Fe}$  is 0.023. On the other hand, secondary ion intensity and mass number ratio of EV54 are distributed uniformly, which is a Pd cathode used in a light water experiment. Depth profiles of Fe standard material are similar to those of EV54.

Sample	Structure of Cathode	Excess Heat	X-ray	Detected Elements	mass57/ mass56
EV50	Pd400Å CaO/Pd 1000Å	Generation (max 3.2W)	X 1 : Background X2.X3: Simultaneous Detection X2(6.6σ <sub>X2</sub> ), X3(6.2σ <sub>X3</sub> )	Si, Fe, Cu	0.036 0.038 0.065
EV51	Pd400Å CaO/Pd 3000Å	Generation (max 1.5W)	X 1 : Background X2.X3: Simultaneous Detection X2(6.4σ <sub>X2</sub> ), X3(7.8σ <sub>X3</sub> )	Fe, Cu	0.24
EV52	Pd400Å CaO/Pd 1000Å	Generation (max 1.9W)	X 1 : Background X2.X3: Simultaneous Detection X2(7.6σ <sub>X2</sub> ), X3(8.8σ <sub>X3</sub> )	Fe, Cu	0.66 0.26 0.22 0.29
EV53	Pd400Å CaO/Pd 3000Å	Generation (max 1.8W)	X 1 : Background X2,X3: Simultaneous Detection X2(14.4σ <sub>X2</sub> ), X3(16.6σ <sub>X3</sub> )	Fe, Cu	0.45 0.37 0.66
EV61	Pd400Å CaO/Pd 1000Å	Generation (max 2.3W)	X 1 : Background X2.X3: Simultaneous Detection X2(6.4σ <sub>X2</sub> ), X3(6.7σ <sub>X3</sub> )	Fe, Au, Cu	0.097
EV54	Pd only (light water)	None (<3σ <sub>H</sub> )	X1, X2, X3: Background	Fe	0.030 0.030
Fe Standard Material		-----	-----	-----	0.023 0.023 0.022

Let us consider the relation between mass57/mass56 and  $^{57}\text{Fe}/^{56}\text{Fe}$ . If we substitute 0.036 of EV50 into mass57/mass56, we obtain

$$\frac{\text{mass57}}{\text{mass56}} = \frac{{}^{57}\text{Fe} + {}^{56}\text{FeH} + {}^{40}\text{Ca}^{16}\text{OH}}{{}^{56}\text{Fe} + {}^{40}\text{Ca}^{16}\text{O}} = \frac{{}^{57}\text{Fe}}{{}^{56}\text{Fe} + {}^{40}\text{Ca}^{16}\text{O}} + \frac{{}^{56}\text{FeH}}{{}^{56}\text{Fe} + {}^{40}\text{Ca}^{16}\text{O}} + \frac{{}^{40}\text{Ca}^{16}\text{OH}}{{}^{56}\text{Fe} + {}^{40}\text{Ca}^{16}\text{O}} = 0.036$$

where all the symbols of the elements mean secondary ion intensity. Every term is positive, therefore

$$\frac{{}^{56}\text{FeH}}{{}^{56}\text{Fe} + {}^{40}\text{Ca}^{16}\text{O}} < 0.036 \quad \frac{{}^{40}\text{Ca}^{16}\text{OH}}{{}^{56}\text{Fe} + {}^{40}\text{Ca}^{16}\text{O}} < 0.036$$

$$\frac{\text{mass57}}{\text{mass56}} < \frac{{}^{57}\text{Fe}}{{}^{56}\text{Fe} + {}^{40}\text{Ca}^{16}\text{O}} + 0.036 + 0.036 < \frac{{}^{57}\text{Fe}}{{}^{56}\text{Fe}} + 0.072$$

$$\therefore \frac{{}^{57}\text{Fe}}{{}^{56}\text{Fe}} > \frac{\text{mass57}}{\text{mass56}} - 0.072$$

If we assume that the effects of Ca are the same as EV50, then  $^{57}\text{Fe}/^{56}\text{Fe}$  of EV52

is larger than 0.15.  $^{57}\text{Fe}/^{56}\text{Fe}$  of EV53 is larger than 0.30.

According to the Table 1, we may say that  $^{57}\text{Fe}/^{56}\text{Fe}$  ratios of EV51, 52 and 53 are anomalously large. The large  $^{57}\text{Fe}/^{56}\text{Fe}$  ratio and the anomalous behavior of SIMS data in Figure 5 indicated that the detected Fe atoms are not produced by normal chemical process. Therefore it is strongly suggested that nuclear reactions occur on the multi-layer cathodes.

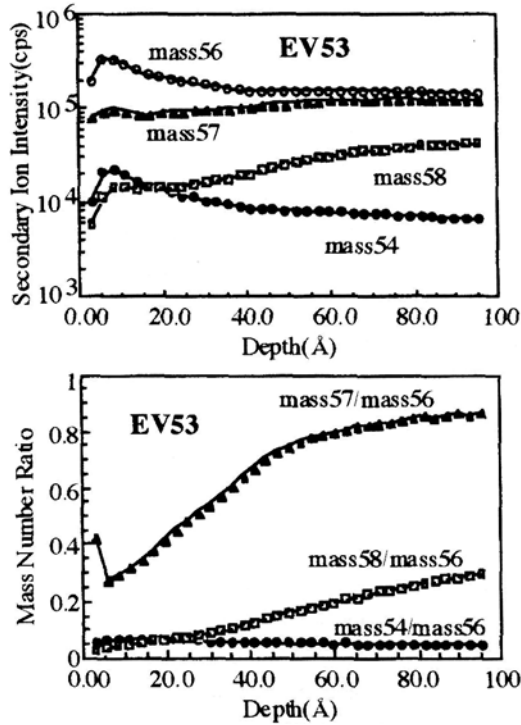


Fig.5 Depth Profiles of Mass Numbers Related to Fe isotopes (EV53:multi-layer cathode)

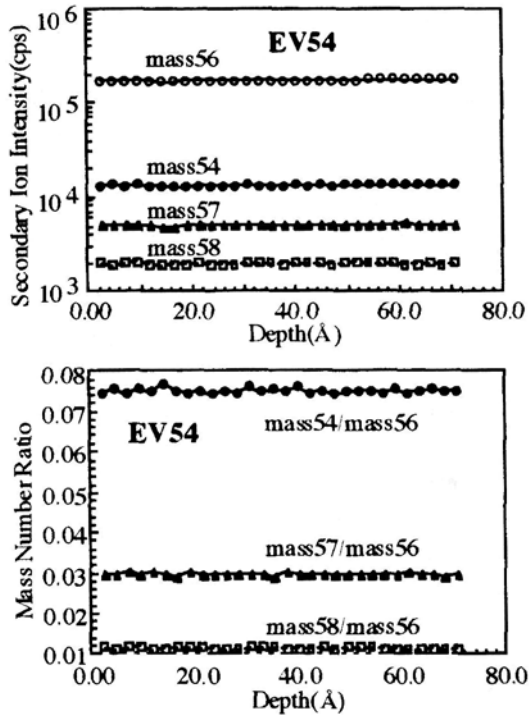


Fig. 6 Depth Profiles of Mass Numbers Related to Fe isotopes (EV54: Pd cathode, light water)

#### References

1. Y. Iwamura, T. Itoh and I. Toyoda, Trans. Fusion Technol., 26, 4T, Part2, 160 (1994)
2. T. Itoh et al, Proc. of ICCF-5, Monte Carlo, Monaco, April 9-13, 1995, p. 189.
3. T. Itoh et al, Proc. of ICCF-6, Toya, Japan, October 13-18, 1996, p.410
4. Y. Iwamura et al, Proc. of ICCF-5, Monte Carlo, Monaco, April 9-13, 1995, p. 197
5. Y. Iwamura et al, Proc. of ICCF-6, Toya, Japan, October 13-18, 1996, p. 274
6. Y. Iwamura et al, Fusion Technology, vol.33, July, 1998, to be published.
7. T. Mizuno et. al, Proc. of ICCF-6, Toya, Japan, October 13-18, 1996, p. 665
8. T. Ohmori et. al, Proc. of ICCF-6, Toya, Japan, October 13-18, 1996, p. 670
9. G. H. Miley et. al, Proc. of ICCF-6, Toya, Japan, October 13-18, 1996, p. 679